

DNA Interaction, Photocleavage and Topoisomerase I Inhibition by Ru(II) Complex with a New Ligand Possessing Phenazine Unit

Xue-Wen Liu¹ · You-Ming Shen¹ · Jun-Shi Shu¹ · Yang Xiao¹ · Song-Bai Zhang¹ · Ji-Lin Lu¹

Received: 29 May 2015 / Accepted: 6 August 2015 / Published online: 19 August 2015
© Springer Science+Business Media New York 2015

Abstract A new ruthenium complex with a dppz-like ligand pyidppz, $[\text{Ru}(\text{bpy})_2(\text{pyidppz})]^{2+}$ (pyidppz = 2-(pyridine-2-yl)imidazo-[4,5-*b*]dipyrido-[3,2-*a*:2',3'-*c*]phenazine) has been synthesized and characterized by ES-MS, elemental analysis, ¹H NMR. Intercalative mode of the complex bound to calf thymus DNA has been supported by different spectroscopic methods and viscosity measurements. The introduction of phenazine unit may be one of the main reasons for the weak emission of Ru(II) complex in aqueous solution. Under irradiation, this complex can efficiently cleave DNA. And the photocleavage reaction of the complex is found to be inhibited in the presence of singlet oxygen scavenger. Topoisomerase inhibition and DNA strand passage assay demonstrated that $[\text{Ru}(\text{bpy})_2(\text{pyidppz})]^{2+}$ and its parent complex $[\text{Ru}(\text{bpy})_2(\text{pyip})]^{2+}$ (pyip = 2-(pyridine-2-yl)imidazo[4,5-*f*][1,10]phenanthroline) can act as efficient catalytic inhibitor of DNA topoisomerase I.

Keywords Ru(II) complex · DNA-binding · Photocleavage · Topoisomerase inhibition

Electronic supplementary material The online version of this article (doi:10.1007/s10895-015-1644-8) contains supplementary material, which is available to authorized users.

✉ Xue-Wen Liu
liuxuewen050@sina.com

✉ You-Ming Shen
ymshen79@163.com

¹ College of Chemistry and Chemical Engineering, Hunan University of Arts and Science, ChangDe 415000, People's Republic of China

Introduction

During the past decades, many ruthenium(II) complexes with polypyridyl ligands have been designed to develop DNA molecular “light switches” due to their possible applications such as detection of DNA base mismatches [1], molecular-scale logic gates, DNA sensing, the signaling of DNA protein binding [2–5] and luminescent probes of DNA structure [6]. These complexes with DNA “light switches” behavior usually exhibit negligible background emission in aqueous solution but display strong luminescence after binding to DNA in intercalation mode [1, 7–18]. An important complex of this type is $[\text{Ru}(\text{bpy})_2\text{dppz}]^{2+}$ (dppz = dipyrido[3,2-*a*:2',3'-*c*]phenazine), whose “light switch” effect involves the protonation of the phenazine nitrogens in excited-state [7, 19]. So it is necessary for Ru(II)-dppz system with “light switch” behavior to protect the phenazine unit from solvent molecular. Several recent reports show that some ruthenium(II) complexes exhibit “light switch” effect similar to $[\text{Ru}(\text{bpy})_2\text{dppz}]^{2+}$, such as $[\text{Ru}(\text{bpy})_2(\text{tpphz})]^{2+}$ [6, 17, 18], $[\text{Ru}(\text{bpy})_2(\text{tapt})]^{2+}$ [18], $[\text{Ru}(\text{phen})_2(\text{dppz-idzo})]^{2+}$ [12, 13], $[\text{Ru}(\text{phen})_2(\text{phehat})]^{2+}$ [20], $[\text{Ru}(\text{bpy})_2(\text{pidbp})]^{2+}$ [15], $[\text{Ru}(\text{bpy})_2(\text{btppz})]^{2+}$ [9] (bpy = 2, 2'-bipyridine; phen = 1,10-phenanthroline; tpphz = tetrapyrido[3,2-*a*:2',3'-*c*:3'',2''-*h*:2''',3'''-*j*]phenazine; dppz-idzo = dipyrido[3,2-*a*:2',3'-*c*]phenazine-10,11-imidazolone; tapt = 4,5,9,18-tetraazaphenanthrene[9,10-*b*] triphenylene; phehat = 1,10-phenanthroline[5,6-*b*]1,4,5,8,9,12-hexaazatriphenylene; pidbp = 2-(pyridine-2-yl)-1-*H*-imidazo[4,5-*i*]dibenzo[2,3-*a*:2',3'-*c*]phenazine; btppz = benzo[*h*]tripyrido[3,2-*a*:2',3'-*c*:2'',3''-*j*]phenazine).

Recently, DNA Topoisomerases has suggested as a possible intracellular target for the design of novel anticancer drugs [21–27]. DNA topoisomerase I is an important enzyme that catalyze a transient single-stranded break of the DNA double helix during DNA relaxation, and critical to both replication

and transcription [28–30]. Several classes of compounds have been reported as Topo I inhibitor, and have been applied to clinical development of anticancer drugs, such as camptothecin families [31], indenoisoquinolines families [32], indolocarbazoles families [33] and phenanthridines families. In recent years, ruthenium complexes have received considerable attention as topoisomerase I inhibitors due to their rich photophysical properties and strong DNA-binding affinities [29, 34–43]. Especially, the DNA intercalative Ru(II) polypyridyl complexes based on $[\text{Ru}(\text{bpy})_2(\text{dppz})]^{2+}$ and $[\text{Ru}(\text{bpy})_2(\text{pip})]^{2+}$ (pip = 2-phenylimidazo[4,5-*f*][1,10]-phenanthroline) have been found to be efficient inhibitor toward DNA Topo I [34–43].

Our group has reported a ruthenium (II) complex $[\text{Ru}(\text{bpy})_2\text{pyip}]^{2+}$ [44] with “light switch” property, whose emission is modulated by Co^{2+} and EDTA. However, this complex emits strong luminescence in aqueous solution, and cannot exhibit DNA “molecular light switch” properties in the presence of only DNA. In order to decrease the emission of this Ru(II) complex in aqueous solution, we intend to modify the pyip ligand by introducing the aromatic ring containing nitrogen atom. So the new ligand pyidppz will possess phenazine unit, which is likely to decrease the emission of the new designed Ru(II) complex $[\text{Ru}(\text{bpy})_2(\text{pyidppz})]^{2+}$ in aqueous solution. In order to gain more information on the DNA-binding, photocleavage properties and DNA topoisomerase I inhibitory activities of this new Ru(II) complex with dppz-like ligand, in this paper, we investigated the emission properties and DNA topoisomerase I inhibitory activities of ruthenium (II) complexes $[\text{Ru}(\text{bpy})_2(\text{pyidppz})]^{2+}$ and $[\text{Ru}(\text{bpy})_2(\text{pyip})]^{2+}$, and their difference were compared. The chemical structures of pyidppz, pyip and ruthenium (II) complex $[\text{Ru}(\text{bpy})_2(\text{pyidppz})]^{2+}$ are given in Scheme 1.

Experimental

Material

The compounds, $[\text{Ru}(\text{bpy})_2(\text{phendione})]^{2+}$ [45], $[\text{Ru}(\text{bpy})_2(\text{pyip})]^{2+}$ [44] and 2-(pyridine-2-yl)-5,6-diamino-1H-benzimidazole [15] were synthesized according to methods in the literature. Calf thymus DNA (CT-DNA) and ethidium bromide were purchased from Sigma (USA). Supercoiled pBR 322 DNA was purchased from MBI Fermentas. DNA topoisomerase I from calf thymus was obtained from Takara. All buffer solutions were prepared using deionized water as follows: (i) buffer A (50 mM NaCl, 5 mM Tris-HCl, pH=7.4); (ii) buffer B (50 mM Tris, 18 mM NaCl, pH=7.8); (iii) buffer C (89 mM Tris, 89 mM boric acid, 2 mM EDTA); (iv) buffer D (50 mM Tris-HCl, 72 mM KCl, 5 mM MgCl_2 , 5 mM DTT, 2 mM sperdine, 0.1 mg/mL BSA, pH=7.5). All DNA-binding experiments were carried out in buffer

A. Buffer B was used to prepare the sample solution for DNA photocleavage. Buffer C (TBE buffer) was used as electrophoresis buffer. Topoisomerase inhibition and DNA strand passage assay were carried out in buffer D. The solutions of CT-DNA in buffer A gave a ratio of UV-vis absorbance of 1.8–1.9:1 at 260 and 280 nm, indicating that the DNA was sufficiently free of protein [17]. The concentration of CT-DNA was determined spectrophotometrically ($\epsilon_{260}=6600 \text{ M}^{-1} \text{ cm}^{-1}$) [46].

Physical Measurement

Microanalysis (C, H and N) were performed with an Elemental Vario EL elemental analyzer. ^1H NMR spectra were recorded on a Bruker ARX-500 spectrometer with $(\text{CD}_3)_2\text{SO}$ for the complexes at 500 MHz at room temperature. Electrospray mass spectra were recorded on a LQC system (Finnigan MAT, USA) using CH_3CN as mobile phase. Absorption spectra were recorded on a Shimadzu UV-2600 spectrophotometer and emission spectra were recorded on a Hitachi F-2500 spectrofluorophotometer at room temperature.

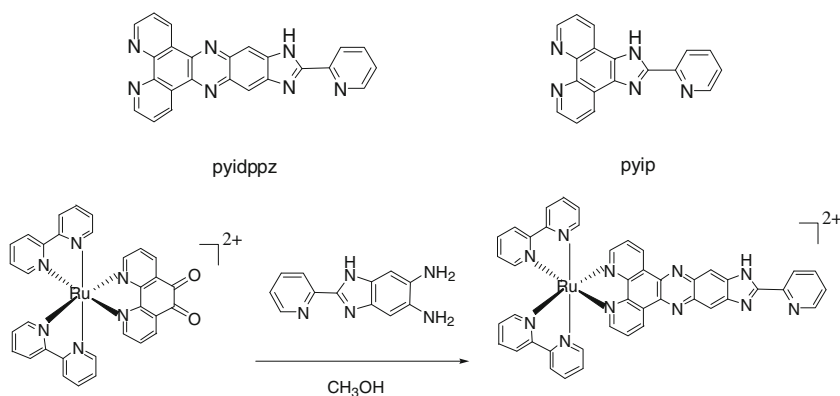
Synthesis of $[\text{Ru}(\text{bpy})_2(\text{pyidppz})](\text{ClO}_4)_2$ (1)

A mixture of 2-(pyridine-2-yl)-5,6-diamino-1H-benzimidazole 0.068 (ca. 0.3 mmol) and $[\text{Ru}(\text{bpy})_2(\text{phendione})](\text{ClO}_4)_2$ 0.247 g (ca. 0.3 mmol) in 20 mL CH_3OH was heated at 65 °C under argon for 8 h. After the reaction was completed, the red solution was cooled to room temperature and poured into 50 mL of water. Methanol was removed on a rotary evaporator. The dark red precipitate was obtained by the addition of NaClO_4 . The crude product was purified by column chromatography on a neutral alumina with acetonitrile-toluene (9:1, v/v) as an eluent. Yield: 0.037 g, 12.2 %. Anal (%):(Found: C, 52.18; H, 2.92; N, 15.20 %. Calcd for $\text{C}_{44}\text{H}_{29}\text{N}_{11}\text{O}_8\text{RuCl}_2$: C, 52.22; H, 2.89; N, 15.23 %). ES-MS (CH_3CN): $m/z=811.6$ ($[\text{M}-2\text{ClO}_4-\text{H}]^+$), 406.1 ($[\text{M}-2\text{ClO}_4]^{2+}$). ^1H NMR (500 MHz, ppm, DMSO-*d*₆): 13.89 (s, 1H), 9.62 (dd, 2H, $J_1=8.0$ Hz, $J_2=7.5$ Hz), 8.91 (t, 5H, $J_1=9.0$ Hz, $J_2=11.0$ Hz), 8.73 (s, 1H), 8.51 (s, 2H), 8.24 (t, 3H, $J_1=8.0$ Hz, $J_2=7.0$ Hz), 8.18 (t, 2H, $J_1=5.5$ Hz, $J_2=3.5$ Hz), 8.15 (t, 2H), 8.03 (t, 1H, $J_1=5.5$ Hz, $J_2=6.0$ Hz), 7.97 (t, 1H, $J_1=6.5$ Hz, $J_2=5.0$ Hz), 7.85 (m, 4H), 7.70 (t, 1H, $J_1=5.5$ Hz, $J_2=6.0$ Hz), 7.63 (t, 2H, $J_1=6.5$ Hz, $J_2=6.5$ Hz), 7.43 (t, 2H, $J_1=7.0$ Hz, $J_2=6.5$ Hz).

DNA-Binding and Photocleavage Experiments

The absorption spectra titrations of Ru(II) complex (20 μM) in buffer A were performed at room temperature to determine the DNA-binding affinities and provide important information for DNA-binding mode. Ruthenium-DNA solution was allowed to incubate for 5 min before the spectra were recorded. The

Scheme 1 The structure of ligands pyip and pyidppz and the synthetic routes of Ru(II) complexes $[\text{Ru}(\text{bpy})_2(\text{pyidppz})]^{2+}$



intrinsic binding constant K of the complex bound to DNA was calculated according to Eq. 1a and 1b [47].

$$(\varepsilon_a - \varepsilon_f) / (\varepsilon_b - \varepsilon_f) = (b - (b^2 - 2K^2 C_t [\text{DNA}] / s)^{1/2}) / 2KC_t \quad (1a)$$

$$b = 1 + KC_t + K[\text{DNA}] / 2s \quad (1b)$$

Where ε_a is the extinction coefficient observed for the $^1\text{MLCT}$ (metal-to-ligand charge transfer) absorption band at a given DNA concentration, ε_f is the extinction coefficient of the complex in the absence of DNA, ε_b is the extinction coefficient of the complex fully bound to DNA. K is the equilibrium binding constant in M^{-1} , C_t is the total metal complex concentration, $[\text{DNA}]$ is the concentration of DNA in M (nucleotide), and s is the binding site size. The experimental absorption titration data were fitted to obtain the binding constants by a non-linear least-square method.

DNA viscosities were measured using an Ubbelohde viscometer maintained at 30.0 ± 0.1 °C in a thermostatic bath. The DNA viscosity was calculated according to $\eta_i = (t_i - t_0) / t_0$, where η_i is the corresponding values of DNA viscosity; t_i is the flow time of the solutions in the presence or absence of the complex; and t_0 is the flow time of buffer alone. Data were presented as $(\eta/\eta_0)^{1/3}$ vs. binding ratio [8], where η is the viscosity of DNA in the presence of complex and η_0 is the viscosity of DNA alone.

The competitive binding experiments were performed by titrating the samples containing 5 μM ethidium bromide (EB) and 100 μM DNA in buffer A with increasing concentration of Ru(II) complex. The EB-DNA solution was incubated for 4 h before use. All the samples were excited at 515 nm, and emission spectra were recorded in the region 530–700 nm.

For the gel electrophoresis experiments, supercoiled pBR322 DNA (0.1 μg) was treated with Ru(II) complex in buffer B, and the solutions were incubated for 1 h in the dark, then irradiated at room temperature with an UV lamp (365 nm, 10 W). The samples were analyzed by electrophoresis for 2 h at 75 V in buffer C containing 1 % agarose gel. The gel was stained with 1.0 $\mu\text{g}\cdot\text{mL}^{-1}$ ethidium bromide and then photographed under UV light.

Topoisomerase I Inhibition Assay

The enzymatic activities of Topo I for Ru(II) complexes were monitored by relaxation of supercoiled pBR322 DNA. The IC_{50} values (50 % inhibitory concentrations) were obtained by the relaxation assay. For the relaxation assay, the reaction mixture (10 μL) contained 0.1 μg pBR322 DNA, 1U Topo I, Ru(II) complexes and buffer D. After incubation at 37 °C for 30 min, the reaction was stopped by addition of 2 μL loading buffer 0.25 % bromophenol blue, 4.5 % sodium dodecyl sulfate, and 45 % glycerol. Agarose gel (1 %) was used for electrophoresis in buffer C as described in the section on DNA photocleavage.

DNA Strand Passage Assay

To test whether the Ru(II) complexes interfere with the DNA relaxation reaction by inhibiting Topo I catalysis or by altering the apparent topological state of DNA, the DNA strand passage assay was performed. Reaction mixture contained 0.3 μg pBR322 DNA, 30 μM drug and 5 U Topo I in buffer D (total volume = 40 μL). After a 5 min incubation of DNA with 30 μM Ru(II) complex or EB, Topo I was added, and the reaction mixture were incubated up to different time at 37 °C. Reactions were stopped and subjected to electrophoresis as described above.

Results and Discussion

Synthesis and Characterization

The outline of the synthesis of the complex $[\text{Ru}(\text{bpy})_2(\text{pyidppz})]^{2+}$ is presented in Scheme 1. The mononuclear ruthenium(II) complex is synthesized by the condensation of 2-(pyridine-2-yl)-5,6-diamino-1H-benzimidazole with the precursor complex $[\text{Ru}(\text{bpy})_2(\text{phendione})]^{2+}$ in methanol, because the the ligand pyidppz can coordinate metal ion via two different sites. The desired Ru(II) complex **1** was

purified by column chromatography, and characterized by element analysis, ES-MS and ^1H NMR. In the ESI-MS spectra for Ru(II) complex **1**, two signals of $[\text{M}-2\text{ClO}_4-\text{H}]^+$ and $[\text{M}-2\text{ClO}_4]^{2+}$ were observed. And the doubly charged species appeared as major peak. The measured molecular weights were consistent with expected values. The Ru(II) complex, $[\text{Ru}(\text{bpy})_2(\text{pyidppz})]^{2+}$ displayed resolvable ^1H NMR spectra (Fig. S1), and all proton chemical shifts were assigned based on the comparison with those of similar compounds [7–18, 36–44]. A singlet peak for the complex appears at *ca.* 13.9, which assigned to the proton on the nitrogen atom of the imidazole. This proton can be seldomly observed for $[\text{Ru}(\text{bpy})_2(\text{pip})]^{2+}$ and its derivatives due to the quickly exchanges between the two nitrogens of the imidazole ring. Chao et al. also reported that the proton on the nitrogen atom of the imidazole resonated at *ca.* 13.9 for $[\text{Ru}(\text{bpy})_2(\text{icip})]^{2+}$ [40].

Electronic Absorption Titration

The application of absorption titration in DNA binding studies is one common optical method. When a probe bound to DNA via intercalation, changes in the absorption spectra (hypochromism and bathochromism) will occur due to the intercalation mode involving a strong π - π stacking interaction between aromatic chromophore and the base pairs of DNA. The extent of the hypochromism commonly depends on the intercalative binding strength.

The electronic absorption spectra of $[\text{Ru}(\text{bpy})_2(\text{pyidppz})]^{2+}$ were measured in buffer A at room temperature. In the absorption spectra of the complex, the band at 288 nm for **1** is assigned to bpy-centered π - π^* transitions in comparison with $[\text{Ru}(\text{bpy})_3]^{2+}$. The band in the range of 300–400 nm can be ascribed to intraligand (IL) π - π^* transitions and a broad band at the lowest energy at 421 nm for **1** is attributed to MLCT transition. Figure 1 shows the changes in the absorption spectra of complex **1** in the absence and presence of CT-DNA ($[\text{Ru}] = 20 \mu\text{M}$). As the DNA concentrations gradually increased, the obvious decrease in the absorptivity (hypochromism) was observed for the complex. For complex **1**, the hypochromism in the MLCT band reaches about 15.2 % at 421 nm at a ratio of $[\text{DNA}]/[\text{Ru}] = 7.5$. The hypochromicity of Ru(II) complex suggested that there is some interaction between the complex and DNA.

To quantify DNA affinity of $[\text{Ru}(\text{bpy})_2(\text{pyidppz})]^{2+}$, the changes of the $^1\text{MLCT}$ absorbance at 421 nm for complex **1** can be used to obtain the DNA binding constant K according to Eq. 1 [47]. The intrinsic binding constant K obtained for complex **1** is $2.4 \pm 0.1 \times 10^5 \text{ M}^{-1}$ ($s = 0.74$). The value is smaller than that of the parent complexes, $[\text{Ru}(\text{bpy})_2(\text{dppz})]^{2+}$ ($3.2 \times 10^6 \text{ M}^{-1}$) [48] and $[\text{Ru}(\text{bpy})_2(\text{pyip})]^{2+}$ ($5.3 \times 10^5 \text{ M}^{-1}$) [44]. Our previous report showed that $[\text{Ru}(\text{bpy})_2(\text{pyip})]^{2+}$ exhibited lower DNA affinity than that of $[\text{Ru}(\text{bpy})_2(\text{dppz})]^{2+}$. This may

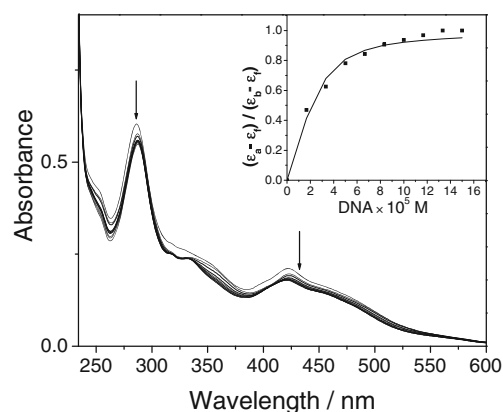


Fig. 1 Absorption spectra of Ru(II) complex **1** in buffer A upon the addition of CT-DNA, $[\text{Ru}] = 20 \mu\text{M}$, $[\text{DNA}] = 0\text{--}150 \mu\text{M}$. Arrow shows the absorbance changing upon the increase in DNA concentration. Inset: plots of $(\epsilon_a - \epsilon_f) / (\epsilon_b - \epsilon_f)$ vs. $[\text{DNA}]$ for the titration of DNA to Ru(II) complex

be attributed to the different planarity of the intercalative ligand. Here, the lower DNA affinity of $[\text{Ru}(\text{bpy})_2(\text{pyidppz})]^{2+}$ may be due to the steric hindrance of pyidppz in spite of the larger planar area of the pyidppz ligand. From the above results, we could deduce that the complex binds to DNA with high DNA affinity. However, the DNA binding mode cannot be determined exclusively using optical method, since surface aggregation leads to similar results. Further investigations are needed to elucidate the DNA-binding mode of the complex.

Emission Spectra Studies

The Emission spectroscopy is one of the most common and sensitive optical methods to study drug-DNA interaction and may give important information for the DNA-binding mode. The result of the emission titration of the complex with DNA was shown in Fig. 2. In buffer A, complex **1** shows very weak fluorescence in the absence of DNA at 600 nm. Compared the emission intensity of complex **1** with that of its parent complex $[\text{Ru}(\text{bpy})_2(\text{pyip})]^{2+}$ (only 2.03 % of the emission intensity of $[\text{Ru}(\text{bpy})_2(\text{pyip})]^{2+}$) (Fig. S2), the weak fluorescence of $[\text{Ru}(\text{bpy})_2(\text{pyidppz})]^{2+}$ may be due to the introduction of phenazine unit. Upon the addition of CT-DNA, the emission is enhanced by a factor of *ca.* 5.10 for complex **1**. Obviously, complex **1** can act as DNA “molecular light switch”. The emission enhancement may be due to the protection of the phenazine nitrogens from solvent. From the fluorescence titration results, we also induced that the complex can strongly interact with DNA and be protected by DNA efficiently, since the hydrophobic environment inside the DNA helix reduces the accessibility of solvent water molecules to the complex and the complex mobility is restricted at the binding site, and this will lead to the decrease of vibration modes of relaxation.

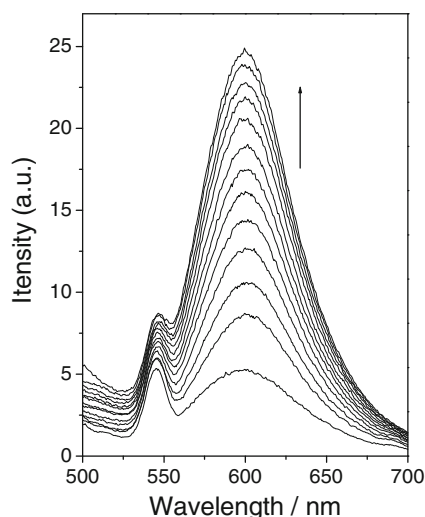


Fig. 2 Fluorescence spectra of Ru(II) complex (5 μM) **1** in buffer A at 298 K in the absence and the presence of CT-DNA. Arrow shows the intensity change upon the increase in DNA concentration

The EB competitive binding experiments is a well-established assay based on the displacement of the intercalating drug EB from CT-DNA, and may provide more information about the DNA-binding mode and the DNA affinities of the complex. Due to the weak fluorescence for free EB, the Ru(II) complex $[\text{Ru}(\text{bpy})_2(\text{pyidppz})]^{2+}$ and DNA-bound Ru(II) complex on the excitation at 515 nm, their emission has little influence on EB competitive binding experiment. Figure 3 shows fluorescence quenching spectra of DNA-bound EB by Ru(II) complex. Upon the addition of Ru(II) complex, sharp decrease was observed in EB emission intensities, indicating the complex could displace EB from DNA. From data in Fig. 3, in the plot of percentage of quenching fluorescence, $(I_0 - I)/I_0$ versus $[\text{Ru}]/[\text{EB}]$, we can see that 50 % EB molecules were displaced from adjacent DNA base pairs at a concentration ratio of $[\text{Ru}]/[\text{EB}] = 6.00$ for complex **1**. By taking the DNA binding constant of $1.4 \times 10^6 \text{ M}^{-1}$ for EB

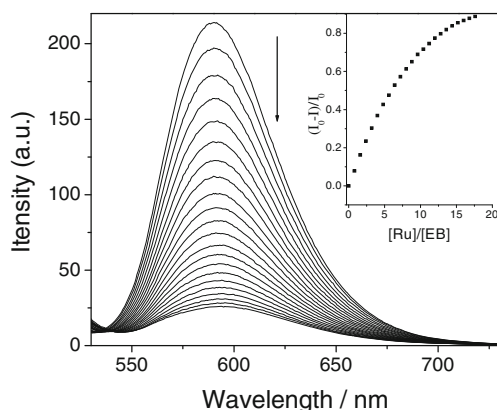


Fig. 3 Fluorescence quenching spectra of DNA-bound EB by Ru(II) complex **1**, $[\text{DNA}] = 100 \mu\text{M}$, $[\text{EB}] = 5 \mu\text{M}$. Arrow shows the intensity change upon increasing Ru(II) complex concentration. Inset: plots of relative integrated fluorescence intensity vs. $[\text{Ru}]/[\text{EB}]$

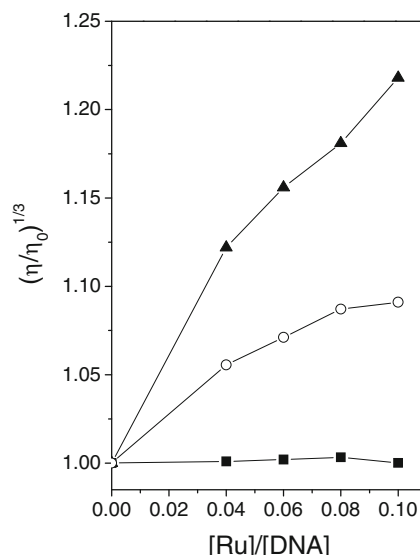


Fig. 4 Effects of the increase in amounts of EB (black triangle), $[\text{Ru}(\text{bpy})_2(\text{pyidppz})]^{2+}$ (white circle) and $[\text{Ru}(\text{bpy})_3]^{2+}$ (black square) on the relative viscosity of CT-DNA at 30 (± 0.1) °C, respectively. The total concentration of DNA is 0.25 mM

[49, 50], the apparent DNA binding constant K_{app} value of the Ru(II) complex was calculated according to Eq. 2 [51].

$$K_{app} = K_{EB}([\text{EB}]_{50\%}/[\text{Ru}]_{50\%}) \quad (2)$$

where K_{app} is the apparent DNA binding constant of the Ru(II) complex, K_{EB} is the DNA binding constant of EB, and $[\text{EB}]_{50\%}$ and $[\text{Ru}]_{50\%}$ are the EB and Ru(II) complex concentrations at 50 % fluorescence, respectively. The value was derived to be $2.33 \times 10^5 \text{ M}^{-1}$ for complex **1**, which is similar to the intrinsic binding constant K value derived from the absorption titration data. This result thus confirms that Ru(II) complex may bind to DNA through intercalation and exhibit higher DNA-binding affinities.

Viscosity Properties

To further clarify the DNA-binding properties and the binding mode of the present complex, the viscosity measurements were carried out on CT-DNA by varying the concentration of the added complex. It is well known that the DNA viscosity measurement is a useful means of determining whether a complex intercalate into DNA. A classical intercalative binding would cause elongation of the DNA helix as base pairs are separated to accommodate the bound ligand, resulting in the increase of DNA viscosity. In contrast, a partial, non-classical

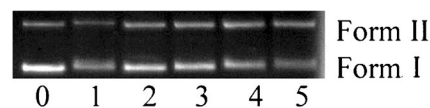


Fig. 5 Photoactivated cleavage of pBR322 DNA in the presence of Ru(II) complexes after 2 h irradiation at 365 nm. Lane 0, DNA alone; Lane 1, Ru+DNA, no hv; Lanes 2–5: complex at 10, 20, 40 and 60 μM

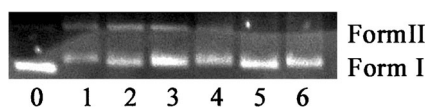


Fig. 6 Agarose gel showing Cleavage of pBR322 DNA incubated with Ru(II) complex **1** (40 μM) and different inhibitors after 2 h irradiation at 365 nm. Lane 0: DNA alone, lane 1: DNA + Ru, lane 2–6: DNA + Ru + 1 M DMSO, 100 mM mannitol, 1000 $\text{U}\cdot\text{mL}^{-1}$ SOD, 25 mM NaN_3 , 1.2 mM histidine

intercalation of the ligand could bend (or kink) the DNA helix, resulting in the decrease of DNA viscosity [52–54]. In addition, electrostatic binding mode has little effect on DNA viscosity.

The effect upon addition EB, complex **1** and $[\text{Ru}(\text{bpy})_3]^{2+}$ on the CT-DNA viscosity are shown in Fig. 4. With increasing amount of Ru (II) complex **1**, the relative viscosities of CT-DNA increases steadily. Ethidium bromide (EB), as a typical intercalator, can increase the relative DNA viscosity for lengthening of the DNA double helix through intercalative binding. While complex $[\text{Ru}(\text{bpy})_3]^{2+}$, which bind to DNA in an electrostatic binding mode, has little effect on DNA viscosity. The increased degree of DNA viscosity, which may depend on the DNA binding mode and affinity, follows the order of $\text{EB} > \mathbf{1} > [\text{Ru}(\text{bpy})_3]^{2+}$. The results suggest that the complex could bind to DNA through intercalative binding mode.

Photocleavage of pBR 322 DNA by Ru(II) Complex

Many Ru (II) complexes with polypyridyl ligands have been found that they can cleave DNA under irradiation, and they have been investigated for potential use in Photodynamic therapy (PDT) agent. Upon irradiation, the effective cleavage activity is attributed to the well-behaved redox-active and photochemical properties of those ruthenium complexes. Most of them, commonly known as “DNA photocleavers”, are activated by light, and generate singlet oxygen ($^1\text{O}_2$), thus induce single-strand or double-strand cleavage of DNA.

Figure 5 shows the ability of Ru(II) complex **1** to induce the photoactivated cleavage of pBR322DNA upon irradiation at 365 nm. As shown in Fig. 5, Control experiment using DNA alone does not show any obvious DNA cleavage (Fig. 5: lane 0). On increasing irradiation concentration, the amount of Form I of pBR322 DNA is decreased, and that of Form II (nicked circular DNA) is increased. $[\text{Ru}(\text{bpy})_2(\text{dppz})]^{2+}$ has been reported that it is difficult to cleave DNA directly due to its short lifetime and low oxidizing ability in excited states. Although complex **1** did not completely convert DNA from

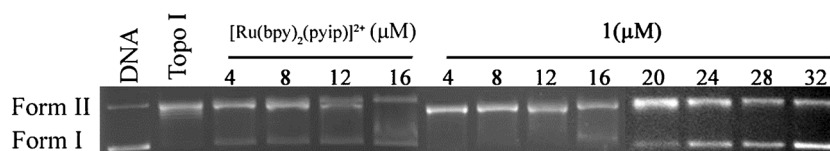
Form I to Form II even when the concentration reached to 60 μM , it still exhibits higher efficiency in DNA-photocleavage than $[\text{Ru}(\text{bpy})_2(\text{dppz})]^{2+}$ [55, 56]. This shows that appropriate modification of Ru-dppz system is help to improve DNA-photocleavage properties of Ru(II)-dppz systems. In addition, there is little difference in DNA-photocleavage properties between $[\text{Ru}(\text{bpy})_2(\text{pyidppz})]^{2+}$ and its parent complex $[\text{Ru}(\text{bpy})_2(\text{pyip})]^{2+}$.

In order to further clarify the mechanism of DNA photocleavage prompted by complex **1**, different potentially inhibiting agents, including hydroxyl radical ($\text{OH}\cdot$) scavengers [46, 57](DMSO and mannitol), singlet oxygen ($^1\text{O}_2$) scavengers [58] (NaN_3 and histidine), and a superoxide anion radical ($\text{O}_2^{\cdot-}$) scavenger (SOD) were introduced to the system. As shown in Fig. 6, scavengers DMSO, mannitol or SOD did not inhibit the cleavage activity of complex **1**, which suggested that hydroxyl radical ($\text{OH}\cdot$) and superoxide anion radical ($\text{O}_2^{\cdot-}$) might be not involved in this DNA photocleavage reaction. However, both NaN_3 and histidine (lane 5, 6) can efficiently inhibit the DNA cleavage activity, suggesting that singlet oxygen ($^1\text{O}_2$) is likely to be the cleaving agent for the DNA photocleavage reaction. Therefore, DNA photocleavage prompted by complex **1** might not occur via an oxidative pathway involving superoxide anion radical ($\text{O}_2^{\cdot-}$) and hydroxyl radical ($\text{OH}\cdot$), but probably via an oxidative process by generating singlet oxygen.

Topoisomerase I Inhibition by Ru(II) Complexes

DNA topoisomerase I is an important nuclear enzyme responsible for the relaxation of supercoiled DNA, the knotting or unknotting of single-stranded circular DNA and the formation of double-strand circular DNA by two single-stranded DNA ring. The effect of Ru(II) complexes on the relaxation activities of Topo I was investigated using negatively supercoiled plasmid DNA as a substrate. The results of the inhibitory effect of two complexes on the catalytic activity of DNA topoisomerase I were shown in Fig. 7. As expected, in the absence of complexes, Topo I completely relaxed negatively supercoiled plasmid DNA, whereas both complexes exhibited different degrees of catalytic inhibition against DNA topoisomerase I at different concentrations. IC_{50} is $\sim 16 \mu\text{M}$ for $[\text{Ru}(\text{bpy})_2(\text{pyip})]^{2+}$ and $\sim 28 \mu\text{M}$ for complex **1**. The IC_{50} value of $[\text{Ru}(\text{bpy})_2(\text{pyip})]^{2+}$ is similar to those of Topo I classical inhibitors and some derivatives of $[\text{Ru}(\text{bpy})_2(\text{pip})]^{2+}$, such as CPT (17 μM) [59], Topostatin (17 μM) [59], $[\text{Ru}(\text{bpy})_2(\text{bfipH})]^{2+}$ (17 μM) [38] and $[\text{Ru}(\text{bpy})_2(\text{appo})]^{2+}$

Fig. 7 Effect of different concentrations of Ru(II) complex **1** and $[\text{Ru}(\text{bpy})_2(\text{pyip})]^{2+}$ on DNA Topo I catalytic activity



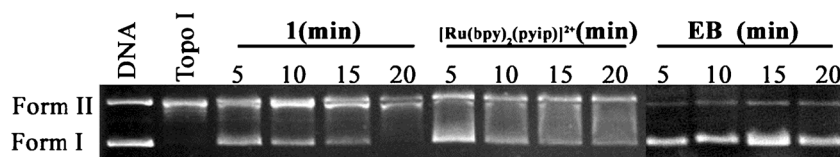


Fig. 8 The time dependence of Topo I DNA strand passage assays in the presence of complex **1**, $[\text{Ru}(\text{bpy})_2(\text{pyip})]^{2+}$ and EB

(25 μM) [37]. Although complex **1** has a similar structure to $[\text{Ru}(\text{bpy})_2(\text{pyip})]^{2+}$, the IC_{50} value of complex **1** is smaller than that of $[\text{Ru}(\text{bpy})_2(\text{pyip})]^{2+}$. These results implied that both complexes could block the DNA strand passage event of the enzyme, and act as catalytic inhibitors of DNA Topo I.

Since intercalative agents can induce constrained negative and unconstrained positive superhelical twists in plasmid DNA, and further alter the apparent topological state of DNA. And Topo I removes only the unconstrained positive supercoils, the negatively supercoiled DNA product would be identical to the topological state of the original plasmid substrate [60]. So, except for Topo I catalysis inhibition, the alteration of the topological state of DNA by DNA intercalative agents appears to inhibit enzyme-catalyzed DNA relaxation. In order to determine which one responsible for Topo I inhibitory activity of two Ru(II) complexes, the DNA strand passage assays were performed. The effects of two Ru(II) complexes on enzyme-catalyzed DNA strand passage were assessed by comparing the rate of relaxation of negatively supercoiled plasmid in the absence of drug to the rate of supercoiling of relaxed plasmid in the presence of 30 μM Ru(II) complexes or EB. As reported before, EB was identical to the rate of Topo I-catalyzed DNA relaxation. Figure 8 indicated that the rate of Topo I-catalyzed DNA supercoiling in the presence of the Ru(II) complexes were lower than the rate of EB. These findings indicate that Ru(II) complexes are catalytic inhibitors of Topo I.

Conclusions

In summary, a novel Ru(II) complex **1**, $[\text{Ru}(\text{bpy})_2(\text{pyidppz})]^{2+}$ has been synthesized and characterized. The DNA-binding and photocleavage properties of the complex have been investigated. The results show that the titled complex can bind to DNA in an intercalative mode, and it can act as DNA (CT-DNA) molecular light switch. Furthermore, the complex is efficient DNA-photocleavers upon irradiation at 365 nm, revealing that the appropriate modification of the intercalating ligand dppz can improve DNA photocleavage efficiency of Ru(II)-dppz system. Singlet oxygen ($^1\text{O}_2$) is likely to be the reactive species responsible for the DNA photocleavage. The topoisomerases I inhibitions by the synthesized complexes have been studied.

Acknowledgments We are grateful to the supports of the National Natural Science Foundation of China (21205039, 21342012), the Natural Science Foundation of Hunan Province (13JJ6071, 14JJ7073), the experiment project of Undergraduate Innovative Training Center in Hunan province (Materials Science and Engineering) (15YCYD02) and the construct program of the key discipline in Hunan province (Applied Chemistry).

References

- Friedman AE, Chambron JC, Sauvage JP, Turro NJ, Barton JK (1990) A molecular light switch for DNA: $\text{Ru}(\text{bpy})_2(\text{dppz})^{2+}$. *J Am Chem Soc* 112:4960–4962
- Ling LS, He ZH, Song GW, Zeng YE, Wang C, Bai CL, Chen XD, Shen P (2001) High sensitive determination of DNA by use of molecular “light switch” complex of $\text{Ru}(\text{phen})_2(\text{dppx})^{2+}$. *Anal Chim Acta* 436:207–214
- Ling LS, He ZK, Chen F, Zeng YE (2003) Single-mismatch detection using nucleic acid molecular ‘light switch’. *Talanta* 59:269–275
- DeSilva AP, McClenaghan ND (2004) Molecular-scale logic gates. *Chem Eur J* 10:574–586
- Jiang Y, Fang X, Bai C (2004) Signaling aptamer/protein binding by a molecular light switch complex. *Anal Chem* 76:5230–5235
- Tysoe SA, Kopelman R, Schelzig D (1999) Flipping the molecular light switch Off: formation of DNA-bound heterobimetallic complexes using $\text{Ru}(\text{bpy})_2\text{tpphz}^{2+}$ and transition metal ions. *Inorg Chem* 38:5196–5197
- Hartshorn RM, Barton JK (1992) Novel dipyrrophenazine complexes of ruthenium (II): exploring luminescent reporters of DNA. *J Am Chem Soc* 114:5919–5925
- Ambrose A, Maiya BG (2000) Ruthenium (II) complexes of 6, 7-dicyanodipyridoquinoxaline: synthesis, luminescence studies and DNA interaction. *Inorg Chem* 39:4256–4263
- Chen YM, Liu YJ, Li Q, Wang KZ (2009) pH- and DNA-induced dual molecular light switches based on a novel ruthenium (II) complex. *J Inorg Biochem* 103:1395–1404
- Zeglis BM, Barton JK (2006) A mismatch-selective bifunctional rhodium-oregon green conjugate: a fluorescent probe for mismatched DNA. *J Am Chem Soc* 128:5654–5655
- Ruba E, Hart JR, Barton JK (2004) $[\text{Ru}(\text{bpy})_2(\text{L})]\text{Cl}_2$: luminescent metal complexes that bind DNA base mismatches. *Inorg Chem* 43:4570–4578
- Yao JL, Gao X, Sun WL, Shi S, Yao TM (2013) $[\text{Ru}(\text{bpy})_2\text{dppz-idzo}]$: a colorimetric molecular light switch and powerful stabilizer for G-quadruplex DNA. *Dalton Trans* 42:5661–5672
- Yao JL, Gao X, Sun WL, Fan XZ, Shi S, Yao TM (2012) A naked-eye on-off-on molecular “light switch” based on a reversible “conformational switch” of G-quadruplex DNA. *Inorg Chem* 51:12591–12593
- Liu Y, Chouai A, Degtyareva NN, Lutterman SA, Dunbar KR, Turro C (2005) Chemical control of the DNA light switch: cycling the switch ON and OFF. *J Am Chem Soc* 127:10796–10797

15. Liu XW, Chen YD, Li L, Lu JL, Zhang DS (2012) DNA-binding and photocleavage studies of ruthenium (II) complexes containing asymmetric intercalative ligand. *Spectrochim Acta A* 86:554–561
16. Liao GL, Chen X, Ji LN, Chao H (2012) Visual specific luminescent probing of hybrid G-quadruplex DNA by a ruthenium polypyridyl complex. *Chem Commun* 48:10781–10783
17. Bolger J, Gourdon A, Ishow E, Launay JP (1996) Mononuclear and binuclear tetrapyrrodo [3,2-a:2',3'-c:3'', 2''-h:2''', 3'''-j] phenazine (tpphz) ruthenium and osmium complexes. *Inorg Chem* 35:2937–2944
18. Pourtois G, Beljonne D, Moucheron C, Schumm S, Kirsch-DeMesmaeker A, Lazzaroni R, Brédas JL (2004) Photophysical properties of ruthenium(II) polyyazaaromatic compounds: a theoretical insight. *J Am Chem Soc* 126:683–692
19. Brennaman MK, Alstrum-Acevedo JH, Fleming CN, Jang P, Meyer TJ, Papanikolas JM (2002) Turning the [Ru(bpy)₂dppz]²⁺ light-switch on and off with temperature. *J Am Chem Soc* 124:15094–15098
20. Moucheron C, Mesmaeker AKD, Choua S (1997) Photophysics of Ru(phen)₂(PHEHAT)²⁺: a novel “light switch” for DNA and photo-oxidant for mononucleotides. *Inorg Chem* 36:584–592
21. Li TK, Liu LF (2001) Tumor cell death induced by topoisomerase-targeting drugs. *Annu Rev Pharmacol Toxicol* 41:53–77
22. Nitiss JL (2009) Targeting DNA topoisomerase II in cancer chemotherapy. *Nat Rev Cancer* 9:338–350
23. Nitiss JL (2009) DNA topoisomerase II and its growing repertoire of biological functions. *Nat Rev Cancer* 9:327–337
24. Leung CH, Zhong HJ, Chan DSH, Ma DL (2013) Bioactive iridium and rhodium complexes as therapeutic agents. *Coord Chem Rev* 257:1764–1776
25. Leung CH, Zhong HJ, Yang H, Cheng Z, Chan DSH, Ma VPY, Abagyan R, Wong CY, Ma DL (2012) A metal-based inhibitor of tumor necrosis factor- α . *Angew Chem Int Ed* 51:9010–9014
26. Pommier Y (2006) Topoisomerase I inhibitors: camptothecins and beyond. *Nat Rev Cancer* 6:789–802
27. Pommier Y (2009) DNA topoisomerase I inhibitors: chemistry, biology, and interfacial inhibition. *Chem Rev* 109:2894–2902
28. Wang JC (1996) DNA topoisomerases. *Annu Rev Biochem* 65:635–692
29. Berger JM, Gamblin SJ, Harrison SC, Wang JC (1996) Structure and mechanism of DNA topoisomerase II. *Nature* 379:225–232
30. Wang JC (2002) Cellular roles of DNA topoisomerases: a molecular perspective. *Nat Rev Mol Cell Biol* 3:430–440
31. Wall ME, Wani MC, Cooke CE, Palmer KH, McPhail AT, Sim GA (1966) Plant antitumor agents. I. The isolation and structure of camptothecin, a novel alkaloidal leukemia and tumor inhibitor from camptotheca acuminata. *J Am Chem Soc* 88:3888–3890
32. Aris SM, Pommier Y (2012) Potentiation of the novel topoisomerase I inhibitor indenoisoquinoline LMP-400 by the cell checkpoint and Chk1-Chk2 inhibitor, AZD7762. *Cancer Res* 72:2153–2154
33. Beretta GL, Zuco V, Perego P, Zaffaroni N (2012) Targeting DNA topoisomerase I with non-camptothecin poisons. *Curr Med Chem* 19:1238–1257
34. Kurtzberg LS, Battle T, Rouleau C, Bagley RG, Agata N, Yao M, Schmid S, Roth S, Crawford J, Krumbholz R, Ewesuedo R, Yu XJ, Wang F, Lavoie EJ, Teicher BA (2008) Bone marrow and tumor cell colony-forming units and human tumor xenograft efficacy of noncamptothecin and camptothecin topoisomerase I inhibitors. *Mol Cancer Ther* 7:3212–3222
35. Chandra M, Sahay AN, Pandey DS, Tripathi RP, Saxena JK, Reddy VJM, Puerta MC, Valerga P (2004) Potential inhibitors of DNA topoisomerase II: ruthenium(II) poly-pyridyl and pyridyl-azine complexes. *J Organomet Chem* 689:2256–2267
36. Gao F, Chao H, Wang JQ, Yuan YX, Sun B, Wei YF, Peng B, Ji LN (2007) Targeting topoisomerase II with the chiral DNA-intercalating ruthenium(II) polypyridyl complexes. *J Biol Inorg Chem* 12:1015–1027
37. Gao F, Chao H, Zhou F, Chen X, Wei YF, Zheng KC, Ji LN (2008) Synthesis, GC selective DNA binding and topoisomerase II inhibition activities of ruthenium(II) polypyridyl complex containing 11-aminopteridino[6,7-f][1,10]phenanthroline-13(12H)-one. *J Inorg Biochem* 102:1050–1059
38. Du KJ, Wang JQ, Kou JF, Li GY, Wang LL, Chao H, Ji LN (2011) Synthesis, DNA-binding and topoisomerase inhibitory activity of ruthenium(II) polypyridyl complexes. *Eur J Med Chem* 46:1056–1065
39. Kou JF, Qian C, Wang JQ, Chen X, Wang LL, Chao H, Ji LN (2012) Chiral ruthenium(II) anthraquinone complexes as dual inhibitors of topoisomerases I and II. *J Biol Inorg Chem* 17:81–96
40. Liao GL, Chen X, Wu J, Qian C, Wang Y, Ji LN, Chao H (2015) Ruthenium (ii) polypyridyl complexes as dual inhibitors of telomerase and topoisomerase. *Dalton Trans*. doi:10.1039/C4DT03585B
41. He XJ, Zeng LL, Yang G, Xie LJ, Sun XN, Tan LF (2013) DNA binding, photocleavage and topoisomerase inhibitory activity of polypyridyl ruthenium(II) complexes containing the same ancillary ligand and different main ligands. *Inorg Chim Acta* 408:9–17
42. He XJ, Jin LH, Tan LF (2015) DNA-binding, topoisomerases I and II inhibition and in vitro cytotoxicity of ruthenium(II) polypyridyl complexes: [Ru(dppz)₂L]²⁺ (L = dppz-11-CO₂Me and dppz). *Spectrochim Acta A* 135:101–109
43. Khan RA, Arjmand F, Tabassum S, Monari M, Marchetti F, Pettinari C (2014) Organometallic ruthenium(II) scorpionate as topoisomerase II α inhibitor; in vitro binding studies with DNA, HPLC analysis and its anticancer activity. *J Organomet Chem* 771:47–58
44. Liu XW, Shen YM, Lu JL, Chen YD, Li L, Zhang DS (2010) Synthesis, DNA-binding and photocleavage of “light switch” complexes [Ru(bpy)₂(pyip)]²⁺ and [Ru(phen)₂(pyip)]²⁺. *Spectrochim Acta A* 77:522–527
45. Goss CA, Abruna HD (1985) Spectral, electrochemical and electrocatalytic properties of 1, 10-phenanthroline-5, 6-dione complexes of transition metals. *Inorg Chem* 24:4263–4267
46. Reichmann ME, Rice SA, Thomas CA, Doty P (1954) A further examination of the molecular weight and size of desoxypentose nucleic acid. *J Am Chem Soc* 76:3047–3053
47. McGhee JD, von Hippel PH (1974) Theoretical aspects of DNA-protein interactions: co-operative and non-cooperative binding of large ligands to a one-dimensional homogeneous lattice. *J Mol Biol* 86:469–489
48. Nair RB, Teng ES, Kirkland SL, Murphy CJ (1998) Synthesis and DNA-binding properties of [Ru(NH₃)₄dppz]²⁺. *Inorg Chem* 37:139–141
49. Waring MJ (1965) Complex formation between ethidium bromide and nucleic acids. *J Mol Biol* 13:269–282
50. LePecq JB, Paoletti C (1967) A fluorescent complex between ethidium bromide and nucleic acids: physical-chemical characterization. *J Mol Biol* 27:87–106
51. Boger DL, Fink BE, Brunette SR, Tse WC, Hedrick MP (2001) A simple, high-resolution method for establishing DNA binding affinity and sequence selectivity. *J Am Chem Soc* 123:5878–5891
52. Satyanarayana S, Dabroniak JC, Chaires JB (1992) Neither DELTA-nor LAMBDA-tris (phenanthroline) ruthenium (II) binds to DNA by classical intercalation. *Biogeosciences* 31:9319–9324
53. Satyanarayana S, Dabroniak JC, Chaires JB (1993) Tris (phenanthroline) ruthenium (II) enantiomer interactions with DNA: mode and specificity of binding. *Biogeosciences* 32:2573–2584
54. Roy M, Pathak B, Patra AK, Jemmins ED, Nethaji M, Chakravarty AR (2007) New insights into the visible-light-induced DNA cleavage activity of dipyrrodoquinoxaline complexes of bivalent 3d-metal ions. *Inorg Chem* 46:11122–11132

55. Sentage C, Chambron JC, Sauvage JP, Pailous N (1994) Tuning the mechanism of DNA cleavage photosensitized by ruthenium dipyridophenazine complexes by varying the structure of the two non intercalating ligands. *J Photochem Photobiol B* 26:165–174
56. Yu HJ, Chao H, Jiang L, Li LY, Huang SM, Ji LN (2008) Single oxygen-mediated DNA photocleavage of a di-bithiazolyl ruthenium (II) complex $[\text{Ru}(\text{btz})_2(\text{dppz})]^{2+}$. *Inorg Chem Commun* 11:553–556
57. Cohen G, Eisenberg H (1969) Viscosity and sedimentation study of sonicated DNA–proflavine complexes. *Biopolymers* 8:45–55
58. Nilsson FR, Merkel PB, Kearns DR (1972) Unambiguous evidence for the participation of singlet oxygen in photodynamic oxidation of amino acids. *Photochem Photobiol* 16:117–124
59. Suzuki K, Uyeda M (2002) Inhibitory properties of antitumor prostaglandins against topoisomerases. *Biosci Biotechnol Biochem* 66:1706–1712
60. Fortune JM, Velea L, Graves DE, Utsugi T, Yamada Y, Osheroff N (1999) DNA topoisomerases as targets for the anticancer drug TAS-103: DNA interactions and topoisomerase catalytic inhibition. *Biogeosciences* 38:15580–15586